

Raise and Peel Models and Pascal's hexagon combinatorics

P. Pyatov

Bogoliubov Laboratory of Theoretical Physics, JINR
141980 Dubna, Moscow Region, Russia

ABSTRACT. The open spin 1/2 XXZ chain is described in terms of the Temperley-Lieb algebra extended by two boundary generators. For specific values of its parameters the algebra comes to a semigroup regime and the model can be attached a stochastic interpretation. The corresponding 3 cases Raise and Peel Models are defined and combinatorial properties of their stationary states are investigated. A relation between 3 cases stationary states is observed which could be reminiscent of a factorization on the level of algebras. Bilinear equalities for some stationary state coefficients are observed. These equalities, called the Pascal's hexagon relations, are considered in the Appendix. Their particular integral and polynomial solutions are constructed.

1 Introduction.

Recently much interest have been attached to surprising manifestation of the ASM (alternating sign matrices) combinatorics in the properties of the ground state of XXZ spin chain at a particular value $\Delta = -1/2$ of its anisotropy [1]. In subsequent investigations [2]–[13] a list of models possessing such property was substantially extended including the dense O(1) loop model, the rotor model and the "raise and peel" model of fluctuating interface. Two important facts are common for these models. First, all they admit purely algebraic description in terms of an appropriate version of a (quotient of) Temperley–Lieb (TL) algebra (see [10]). Second, the TL algebras always come in a very specific semigroup regime, that certainly has to do with the manifestation of the ASM combinatorics. This latter fact was used in [5, 10] to interpret the loop model as a stochastic process and, thus, to attach direct physical interpretation to components of the ground state vector as (unnormalized) rates of a stationary probability distribution.

In the present paper we use boundary extension of the TL algebra to obtain purely algebraic description of XXZ spin chain with open boundary conditions for generic values of its anisotropy and boundary parameters (see Section 2).

We consider then three stochastic processes associated with the algebra at its semigroup point. Following [12] we call them Raise and Peel Models (RPMs). The RPMs were recently investigated both from physical and mathematical viewpoints in [5], [9]–[13]. In addition to these recent investigations we make a comparative analysis of the stationary states of the processes and present numeric conjectures about them (see Section 3)¹

¹An investigation of the whole spectrum of the models will be reported elsewhere [14].

A special comment should be made concerning the paper [13]. There are many intersections in the results discussed here and in that paper. We decide not to avoid overlapping because (a) we use different presentation language and (b) in both cases results were extracted from calculations on computers and so they may be viewed as two mutually approving computer experiments².

During investigation the RPM's stationary states we find out that some of their coefficients satisfy bilinear equalities, called here the Pascal's hexagon relations. A brief investigation of some integral and polynomial solutions of these recurrent relations is reported in the Appendix.

2 Boundary extended Temperley-Lieb algebra

2.1 Definition.

We start with the type *A* Temperley-Lieb (TL) algebra [15] which as it is well known (see [16]) stands behind the $U_q(sl_2)$ symmetric XXZ spin chain. For the chain of L particles the corresponding TL algebra is generated by the unity and a set of $(L - 1)$ elements e_i , $i = 1, \dots, (L - 1)$, subject to relations

$$e_i e_{i \pm 1} e_i = e_i , \quad e_i^2 = (q + q^{-1}) e_i , \quad (2.1)$$

$$e_i e_j = e_j e_i , \quad \forall i, j : |i - j| > 1 . \quad (2.2)$$

Here parameter $q \in \mathbb{C} \setminus \{0\}$ of the algebra is related to the anisotropy parameter $\Delta = -(q + q^{-1})/2$ of the spin chain.

A boundary extension of this algebra is achieved by adding two more generators f_0 and f_L together with the relations

$$e_1 f_0 e_1 = e_1 , \quad e_j f_0 = f_0 e_j , \quad \forall j > 1 , \quad (2.3)$$

$$e_{L-1} f_L e_{L-1} = e_{L-1} , \quad e_j f_L = f_L e_j , \quad \forall j < L - 1 . \quad (2.4)$$

$$f_0^2 = a f_0 , \quad f_L^2 = \bar{a} f_L , \quad f_0 f_L = f_L f_0 , \quad (2.5)$$

where $a, \bar{a} \in \mathbb{C}$. The algebra with one boundary element (either f_0 , or f_L) called the *blob algebra* was analyzed in [17, 18]. The extension of the TL algebra with the two boundary generators was introduced in [11]. Unlike TL and blob algebras it is infinite dimensional and we are going to further extract its finite dimensional quotient. To this end we consider a pair of unnormalized projectors X_L and Y_L . They are defined differently depending on a

²In fact, there is a small discrepancy in results presented in Conjecture 13.

parity of L

$$\begin{aligned} \text{for } L \text{ even: } X_L &:= \prod_{k=0}^{L/2-1} e_{2k+1}, & Y_L &:= f_0 \prod_{k=1}^{L/2-1} e_{2k} f_L; \\ \text{for } L \text{ odd: } X_L &:= f_0 \prod_{k=1}^{(L-1)/2} e_{2k}, & Y_L &:= \prod_{k=0}^{(L-3)/2} e_{2k+1} f_L. \end{aligned} \quad (2.6)$$

In terms of these projectors reduction conditions read

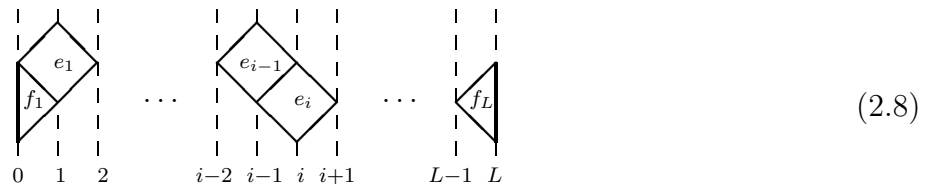
$$X_L Y_L X_L = b X_L, \quad Y_L X_L Y_L = b Y_L. \quad (2.7)$$

The resulting quotient algebra is that one we shall further call the *boundary extended TL algebra*. It is finite dimensional³ and it depends on four parameters q, a, \bar{a} and $b \in \mathbb{C}$.

2.2 Graphical presentation.

There are at least two ways in which the boundary extended TL algebra can be visualized. First one is a straightforward generalization of the diagrammatic realization of the blob algebra presented in [17]. For this one uses familiar "lines and loops" diagrams for the TL generators e_i and realizes the boundary generators f_0 and f_L as two different blobs lying, respectively, on the leftmost and the rightmost lines of the diagram (see [17]). Equivalently, one can draw boundary generator f_0 (f_L) as a half-loop connecting the leftmost (rightmost) line to the boundary (see [11, 13]).

The second way which we are using throughout this paper is the one suitable for modelling of growing interfaces (see [12]). One draws the TL generator e_i as a tile whose diagonal is lying on a vertical line with coordinate i and whose left and right vertices are placed, respectively, on vertical lines with coordinates $i-1$ and $i+1$. The boundary generators f_0 and f_L are drawn as half-tiles with their longest sides lying on vertical lines with coordinates 0 and L , respectively (see Figure below).



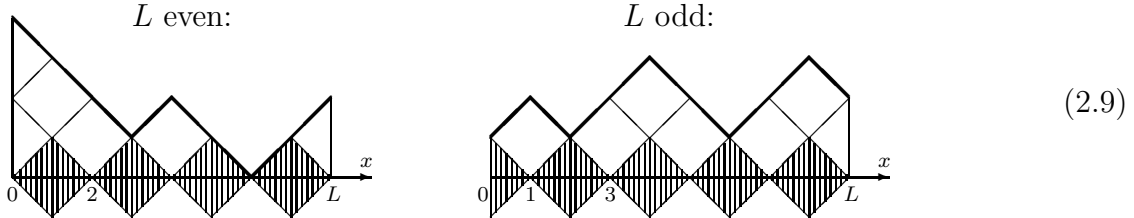
The (half-)tiles can freely move along vertical axes unless they meet their neighbors. Assuming attraction forces acting among the (half-)tiles one represents word in the algebra as a collection of dense polygons built from the (half-)tiles and satisfying following conditions. All polygons are placed between vertical lines with coordinates 0 and L and no vertical line lying between these two boundary verticals crosses the borders of (one or several) polygons in more than two points.

³Dimensions of the boundary extended TL algebras are calculated in an Appendix to [19].

2.3 Relation to XXZ open spin- $\frac{1}{2}$ chain.

Of our main interest is the left ideal in the boundary extended TL algebra generated by X_L ⁴. We denote this ideal as \mathcal{I}_L .

Consider graphical realization of a typical word in the ideal. As we have different definitions of X_L depending on a parity of L , separate pictures for the cases of L even and L odd are given below.



Here we adopt a convention that multiplication from the left by elements e_i , f_0 , or f_L amounts graphically to dropping their respective (half-)tiles up-down. Components of X_L are shown hatched on the pictures.

As it is obvious from pictures (2.9) each word w in the ideal \mathcal{I}_L is uniquely defined by a shape of the upper border $h(w|x)$, $0 \leq x \leq L$, of its corresponding polygon (drawn in bold lines on the pictures). In turn, the border line is suitably encoded by its values at the integer points $h(w|i) := h_i(w)$. $i = 0, 1, \dots, L$. Assuming the height of the tile (= the length of its diagonal) equals 2 and taking the middle line of the bottom row of tiles as a reference axis one gets following prescriptions for a set of $\{h_i\}$

- a) $h_{i+1} - h_i = \pm 1$ and $h_i \geq 0$, $\forall i$;
- b) h_L is an even integer;
- c) there exists i such that $h_i \in \{0, 1\}$.

(2.10)

Here prescription b) relies on our choice of X_L as an ideal generating element. With the choice of Y_L one would constrain h_L to be odd. Prescription c) results from the reduction conditions (2.7).

A line defined by a set $\{h_i\}$ satisfying conditions (2.10) is called *Anchored Cross path* in [20]. A family of such paths contains two famous subfamilies.

- *Ballot paths* are the paths (2.10) with fixed endpoint $h_L = 0$. Their total number is $\binom{L}{[L/2]}$, where $[x]$ is an integer part of x . Examples of Ballot paths are shown on pictures a), b) and c) on Fig. 1 on page 7. Pictures d) and e) there are not the Ballot paths.

⁴Note that in case $b \neq 0$ the element Y_L generates an isomorphic ideal.

- *Dyck paths* are defined for L even and they are fixed at both ends: $h_0 = h_L = 0$. For $L = 2p$ one has $C_p := \frac{1}{p+1} \binom{2p}{p}$ Dyck paths which is the p -th Catalan number. For $L = (2p+1)$ odd close relatives of Dyck paths are those whose endpoints are fixed as $h_0 = 1, h_L = 0$. These paths are in one to one correspondence with the Dyck paths of length $L = (2p+2)$ and later on we will also refer them as Dyck paths. Among the paths shown on Fig. 2 on page 8 cases a), b) and c) are the Dyck paths, while cases d), e), f) are not.

Returning to the Anchored Cross paths one finds their total number being equal 2^L . So we observe that the dimension of the ideal \mathcal{I}_L coincides with the dimension of a representation space of the spin=1/2 chain of L particles. The analogy goes further. It turns out that the ideal \mathcal{I}_L considered as a vector space and supplied with the action of Hamiltonian

$$H_L := \sum_{i=1}^{l-1} (1 - e_i) + c(1 - f_0) + \bar{c}(1 - f_L) \quad (2.11)$$

provides a realization of the open XXZ spin=1/2 chain (further results in this direction will be reported in [14]). Note that the boundary terms of the open chain Hamiltonian carry effectively five independent coefficients which in realization (2.11) are represented by two parameters (c and \bar{c}) of the Hamiltonian and three parameters (a, \bar{a} and b) entering definition of the ideal. The case $c = \bar{c} = 0$ corresponds to $U_q(sl_2)$ symmetric spin chain.

In the rest of the paper we are going to investigate combinatorics of the ground state vector of Hamiltonian (2.11) for the case when the boundary extended TL algebra becomes semigroup

$$q = \exp(i\pi/3), \quad a = \bar{a} = b = 1. \quad (2.12)$$

In this case the Hamiltonian (2.11) becomes an intensity matrix which is appropriate for description of a stochastic process (see, e.g., [10]). Especially, we are interested in three particular cases where parameters c and \bar{c} of the Hamiltonian are chosen as

$$\text{case A: } c = \bar{c} = 0; \quad \text{case B: } c = 1, \bar{c} = 0; \quad \text{case C: } c = \bar{c} = 1. \quad (2.13)$$

Namely in these cases one observes magic manifestation of the ASM combinatorics in properties of the stationary state of the stochastic process (that is given by the ground state vector of the Hamiltonian).

3 Raise and Peel Models with different boundary terms.

3.1 The models definition.

We consider three processes of growth of a film of tiles which are deposited on a one-dimensional substrate of size L .

As a substrate in all cases we choose profiles which are shown hatched on pictures (2.9). A rarefied gas above the substrate contains tiles and (possibly) half-tiles. They are moving along integer vertical lines as illustrated on picture (2.8) and upon hitting the substrate they can be absorbed and form interface configurations as shown on picture (2.9). Depending on a composition of the gas one distinguishes

- case A: the gas contains tiles moving along lines with coordinates $i = 1, 2, \dots, L - 1$; possible interface configurations are given by Dyck paths;
- case B: the gas contains all the tiles and the half-tile moving along 0-th line; possible interface configurations are the Ballot paths;
- case C: the gas contains all the tiles and the half-tiles on both left and right boundaries; possible interface configurations are the Anchored Cross paths.

From discussion of the previous section one infers following translation of data of the processes to a language of the boundary extended TL-algebra:

- the substrate of size $L \longleftrightarrow$ the unnormalized projector X_L ;
- the (half-)tile on i -th vertical line \longleftrightarrow the algebra generators e_i (f_0/f_L for $i = 0/L$);
- interface configurations \longleftrightarrow words in ideal the \mathcal{I}_L generated by X_L ;
- hitting the interface by (half-)tiles \longleftrightarrow left multiplication by e_i (f_0, f_L) in the ideal.

A dynamics of the processes in the algebra language is described by equation

$$\frac{d}{dt} |p_L(t)\rangle = H_L |p_L(t)\rangle. \quad (3.1)$$

Here $|p_L(t)\rangle := \sum_{w \in \mathcal{I}_L} p_L(w|t) w$ is a linear combination of words in the ideal. It may contain all possible words in case C and it is restricted to the subspace of Ballot/Dyck paths in the cases B/A. The coefficient $p_L(w|t)$ has to be a nonnegative real number and it is treated as unnormalized probability to find the system in configuration w at time t . The Hamiltonian H is given by formula (2.11) and the algebra parameters are chosen as in (2.12) to ensure that H is an intensity matrix. The parameters c and \bar{c} of the Hamiltonian for the cases A, B and C are fixed as in (2.13).

Starting from Subsection 3.2 we will concentrate on studying the stationary states of the stochastic processes, those are solutions of equation

$$H_L |p_L\rangle = 0. \quad (3.2)$$

The rest of this Subsection is devoted to a more explicit graphical presentation of dynamics of the processes. We take a viewpoint developed for the case A process in paper [12]. This

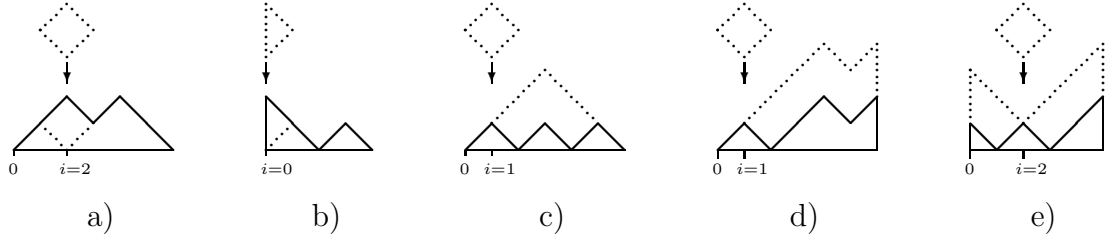


Figure 1: The interface profile before event and the (half-)tiles hitting the interface are drawn in dashed lines. The interface profile after the event is drawn in permanent line. Pictures a) and b) illustrate absorption, respectively, in a bulk and at the boundary of the interface. Pictures c) and d) are examples of avalanches, respectively, in the bulk (number of desorbed tiles $n_d = 3$, size of a substrate $L = 6$) and near the boundary ($n_d = 5$, $L = 6$). Picture e) shows the total avalanche ($n_d = L = 5$).

process was called *raise and peel model* (RPM) there. Cases B and C are versions of the RPM with a different boundary terms. We recall physical (= graphical) interpretation of the RPM evolution (3.1) as described in [12] and adopt it for the cases B and C.

During an infinitesimal time interval dt a single event may happen with equal probability rate at any integer point of the interface. The following events can occur.

- a) At a local minimum point i (that is, if $h_i < h_{i\pm 1}$) the interface either absorbs (half-)tile ($h_i \mapsto h_{i+2}$) with probability dt or it reflects (half-)tile (h_i stays unchanged) with probability $1 - dt$. For the case C there is an exception from this rule described in item d).
- b) At a local maximum point i (that is, if $h_i > h_{i\pm 1}$) the interface always reflects (half-)tiles and stays unchanged.
- c) At a bulk slope point i (that is, $0 < i < L$ and either $h_{i-1} < h_i < h_{i+1}$, or $h_{i-1} > h_i > h_{i+1}$) dropping a tile leads with probability dt to a nonlocal desorption event called avalanche. To describe the avalanche one determines integer k such that for all integers j standing between i and k inequality $h_j > h_i$ holds and either $h_k = h_i$, or k runs out the interval $[0, L]$, i.e., k equals $L + 1$, or -1 . The avalanche causes desorption of one tile at each point j between i and k , that is $h_j \mapsto h_j - 2$. The avalanche size (a number of the desorbed (half-)tiles) $n_d = |i - k| - 1$, $1 \leq n_d \leq L - 1$, measures non-locality of the event.

With probability $1 - dt$ the tile is reflected and the interface stays unchanged.

- d) In case C at a global minimum point i such that $h_i = 1$ and $h_j > h_i$, $\forall j \neq i$, the dropping (half-)tile with probability dt causes the total avalanche of a size $n_d = L$ that is, $h_j \mapsto h_j - 2$, $\forall j \neq i$. Again, with probability $1 - dt$ the (half-)tile is reflected and the interface stays unchanged.

Typical absorption and desorption events are illustrated on Figure 1.

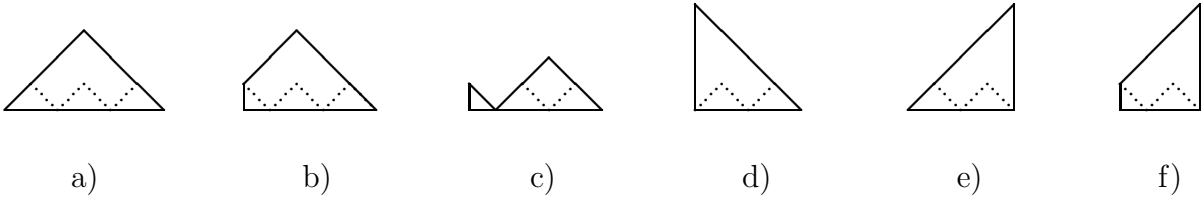


Figure 2: In case A the minimal possible coefficient 1 in null eigenvector stands for pyramid type configuration a) for L even and for configurations b) and c) for L odd. In case B half-pyramid configurations d) has coefficient 1 both for L even and L odd. In case C the minimal coefficient $m_L^{(c)}$ appears again for configurations d) and for e)/f) in case of L even/odd. Dashed lines show the substrate in each case.

3.2 Stationary states: critical values and normalization factor.

Here we present results of a numeric investigation of the stationary states of the raise and peel models. The calculations were carried out with the use of REDUCE program for the system's size up to $L = 13$ in case A, up to $L = 11$ in case B and up to $L = 10$ in case C. In all three cases (2.13) the RPM has a unique stationary state.

Denote components of $|p_L\rangle$ (3.2) in cases A, B and C as $p_L^{(a)}(w)$, $p_L^{(b)}(w)$ and $p_L^{(c)}(w)$, respectively. Here argument w labels in each case relevant interface configurations: those are the sets of Dyck paths $\{w\}_{Dyck}$ in case A, Ballot paths $\{w\}_{Ballot}$ in case B and Anchored Cross paths $\{w\}_{ACross}$ in case C. Since in the semigroup regime the Hamiltonian becomes the intensity matrix one always can choose null eigenvectors $|p_L\rangle$ in such a way that all their components are nonnegative real (see [21]), thus, making the probabilistic interpretation consistent. Moreover, it turns out that no one of coefficients $p_L^{(*)}(w)$ vanishes. So, we can normalize them to be mutually primitive positive integers. Denote their minimal and maximal components as

$$m_L^{(*)} := \min_{\{w\}_*} \{p_L^{(*)}(w)\}, \quad M_L^{(*)} := \max_{\{w\}_*} \{p_L^{(*)}(w)\}. \quad (3.3)$$

It turns out that $m_L^{(a)} = m_L^{(b)} = 1$, but $m_L^{(c)} \neq 1$. The corresponding interface configurations are shown on Fig.(2).

Denote total normalization factors of the stationary probability distributions as

$$S_L^{(*)} := \sum_{\{w\}_*} p_L^{(*)}(w). \quad (3.4)$$

In the table below we collect values of $S_L^{(*)}$ and $m_L^{(c)}$ for $L \leq 11$

| L | 1 | 2 | 3 | 4 | 5 | 6 | 7 | 8 | 9 | 10 | 11 |
|-------------|---|---|----|-----|-------|---------|----------|-------------|----------------|------------------|---------------|
| $S_L^{(a)}$ | 1 | 1 | 2 | 3 | 11 | 26 | 170 | 646 | 7429 | 45885 | 920460 |
| $S_L^{(b)}$ | 1 | 2 | 6 | 33 | 286 | 4420 | 109820 | 4799134 | 340879665 | 42235307100 | 8564558139000 |
| $S_L^{(c)}$ | 2 | 6 | 66 | 858 | 48620 | 1427660 | 47991340 | 11589908610 | 13642004193300 | 1139086232487000 | |
| $m_L^{(c)}$ | 1 | 1 | 2 | 3 | 11 | 13 | 10 | 34 | 323 | 133 | |

(3.5)

The table illustrates clearly the following three conjectures, which were found before in [2, 13].

Conjecture 1. *Let A_n^V (resp., A_n^{VH}) denote a number of vertically symmetric (resp., vertically and horizontally symmetric) alternating sign matrices of a size $n \times n$ ⁵. Then*

$$S_{2p}^{(a)} = A_{2p+1}^V := (-3)^{p^2} \prod_{\substack{1 \leq i \leq p \\ 1 \leq j \leq 2p+1}} \frac{6i - 3j + 1}{2i - j + 2p + 1}, \quad S_L^{(b)} = A_{2L+3}^{VH}. \quad (3.6)$$

Conjecture 2. *Looking at numbers standing in down-up diagonals of the table one observes equalities*

$$S_L^{(b)} = S_L^{(a)} S_{L+1}^{(a)}, \quad (3.7)$$

$$S_L^{(c)} = m_L^{(c)} S_{L+1}^{(b)}. \quad (3.8)$$

The first equality (3.7) allows one to get two expressions for $S_{2p-1}^{(a)}$ ⁶

$$S_{2p-1}^{(a)} = A_{4p-1}^{VH}/A_{2p-1}^V = A_{4p+1}^{VH}/A_{2p+1}^V := \prod_{0 \leq i \leq p-1} \frac{(3i+1)(6i)!(2i)!}{(4i)!(4i+1)!}. \quad (3.9)$$

Their consistency, in turn, is based on relations conjectured in [22]

$$A_{4p+1}^{VH}/A_{4p-1}^{VH} = A_{2p+1}^V/A_{2p-1}^V = \frac{(3p-1)\binom{6p-3}{2p-1}}{(4p-1)\binom{4p-2}{2p-1}}. \quad (3.10)$$

The second equality (3.8) relates quantities $S_L^{(c)}$ and $m_L^{(c)}$. Looking at the table (3.5) one can also assume that $m_L^{(c)}$ are divisors of $S_L^{(a)}$. A formula for $m_L^{(c)}$ refining this simple observation is guessed in [13] (see Eqs.(32), (33) there). That is

$$m_L^{(c)} = \text{Numerator of } \left(\frac{S_L^{(a)}}{S_{L+2}^{(a)}} \right). \quad (3.11)$$

⁵On enumeration of various symmetry classes of alternating sign matrices see [22, 23]

⁶Note that $S_{2p-1}^{(a)}$ is just the number of cyclically symmetric transpose complement plane partitions in a $(2p)^3$ box (see, e.g., [24], p.199). It is usually denoted as $N_S(2p)$.

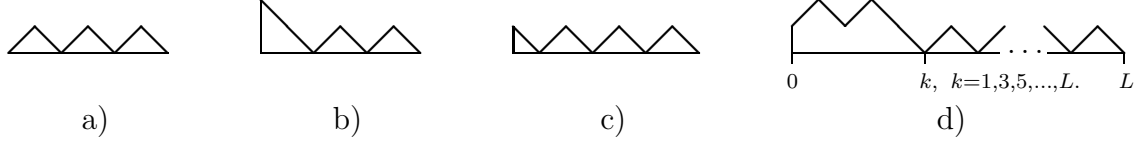


Figure 3: In case A the maximal coefficient in null eigenvector stands for configuration a) for L even and for configurations d) for L odd. In case B configurations a) and b) enter the null eigenvector with the maximal coefficient if L is even and configuration c) corresponds to maximal coefficient if L is odd.

Remark. At this point one may propose another reasonable normalization for the stationary state in case C. Denoting components of the stationary state in this new normalization as $\{\tilde{p}_L^{(c)}\}$ one may fix normalization demanding that

$$\tilde{m}_L^{(c)} := \min_{\{w\}_{ACross}} \{\tilde{p}_L^{(c)}(w)\} = S_L^{(a)}, \quad (3.12)$$

Certainly, the initial normalization is a more economic one and thus it is better suited for calculations. However, normalization (3.12) has an advantage in interpreting results. E.g., formula for the total normalization factors in this case looks as

$$\tilde{S}_L^{(c)} = S_L^{(a)} S_{L+1}^{(b)} = S_L^{(b)} S_{L+2}^{(a)} = S_L^{(a)} S_{L+1}^{(a)} S_{L+2}^{(a)}, \quad (3.13)$$

which is much more in the spirit of eq.(3.7) then the formula (3.8). We decide to keep initial ‘economic’ normalization throughout the text and to comment on the second normalization when presenting results.

The last conjecture of this section describes the most probable components of the stationary states in cases A and B

Conjecture 3. *The maximal coefficient $M_L^{(a)}$ appear in the set $\{p_L^{(a)}\}$ with multiplicity 1 for L even and $(L-1)/2$ for L odd. The maximal coefficient $M_L^{(b)}$ appear in the set $\{p_L^{(b)}\}$ with multiplicity 2 for L even and 1 for L odd. Their corresponding interface configurations are shown on Fig.(3) and values of the maximal coefficients are given by formulas*

$$M_L^{(a)} = S_{L-1}^{(a)}, \quad (3.14)$$

$$M_{L=2p}^{(b)} = (S_L^{(a)})^2, \quad M_{L=2p+1}^{(b)} = S_{L-1}^{(a)} S_{L+1}^{(a)}. \quad (3.15)$$

3.3 Case A: detailed distributions and Pascal’s hexagon relation

Let us first introduce more notation.

An integer point i of an interface configuration $\{h_k\}_{k=0,\dots,L}$ such that $0 < i < L$ in case A; $0 \leq i < L$ in case B; or, $0 \leq i \leq L$ in case C, is called an N -contact if $h_i = N$ and $h_{i\pm 1} = N+1$. The contact points are local minima of the interface at which it can absorb (half-)tiles. For instance, the interface shown on picture d) of Fig.(3) has only one 1-contact $i = 2$ in case A, but it has two 1-contacts $i = 0, 2$ in cases B, or C. In all cases it has 0-contacts at points $k, k+2, \dots, L-2$ and additionally it has 0-contact at point L in case C.

For either of the families of Dyck, Ballot, or Anchored Cross paths we denote $\{w\}_*^N$ (here $*$ stands for an appropriate family name) the subsets of all interface configurations which have no p -contacts with $p < N$. These are the configurations whose global minimum (excluding points 0 and L in case A, or point L in case B) is higher or equal to N . Obviously, one has $\{w\}_*^0 \equiv \{w\}_*$ and $\{w\}_*^{N+1} \subset \{w\}_*^N$. We shall stress that there is no strict correlation between the subsets $\{w\}_*^N$ corresponding to different sets of paths. For example, for any N

$$\{w\}_{Dyck}^N \subset \{w\}_{Ballot}^k, \quad \{w\}_{Dyck}^N \cap \{w\}_{Ballot}^{k+1} = \emptyset,$$

where $k = 0/1$ for L even/odd. This is because the left boundary point $h_0 = 0$, or 1 of a Dyck path is treated as 0-, or 1-contact point in a family of Ballot paths.

Considering the subsets $\{w\}_*^N$ proves to be useful for analysis of the raise and peel model in cases A and B. Here label N spans integers from 0 to $[(L-1)/2]$ in case A and from 0 to $(L-1)$ in case B.⁷ The subset with highest possible N in both cases A and B contains only element which is drawn on Fig.(2), pictures a)/b) and d), respectively. As it was mentioned before, this element enters the stationary state with a minimal coefficient 1. In the sequel we determine detailed distributions $S_{L,N}^{(*)}$ and detailed maxima $M_{L,N}^{(*)}$ for each of the subsets $\{w\}_*^N$

$$S_{L,N}^{(*)} := \sum_{\{w\}_*^N} p_L^{(*)}(w), \quad M_{L,N}^{(*)} := \max_{\{w\}_*^N} \{p_L^{(*)}(w)\}. \quad (3.16)$$

In this section we concentrate on studying the case A. The table below contains values of $S_{L,N}^{(a)}$ for L up to 13.

| $L \setminus N$ | -1 | 0 | 1 | 2 | 3 | 4 | 5 | 6 |
|-----------------|---------|-----------|---------|----------|---------|-------|-----|----|
| 1 | | 1 | | | | | | |
| 2 | 1 | | 1 | | | | | |
| 3 | | 2 | | 1 | | | | |
| 4 | 3 | | 3 | 1 | | | | |
| 5 | | 11 | | 4 | 1 | | | |
| 6 | 26 | | 26 | 5 | 1 | | | |
| 7 | | 170 | | 50 | 6 | 1 | | |
| 8 | 646 | | 646 | 85 | 7 | 1 | | |
| 9 | | 7429 | | 1862 | 133 | 8 | 1 | |
| 10 | 45885 | | 45885 | 4508 | 196 | 9 | 1 | |
| 11 | | 920460 | | 202860 | 9660 | 276 | 10 | 1 |
| 12 | 9304650 | | 9304650 | 720360 | 18900 | 375 | 11 | 1 |
| 13 | | 323801820 | | 64080720 | 2184570 | 34452 | 495 | 12 |
| | | | | | | | | 1 |

(3.17)

For later convenience we add to the table a column for $N = -1$ setting $S_{L=2p,N=-1}^{(a)} := S_{L=2p,N=0}^{(a)}$. We also align data corresponding to even, or odd values of L leftwards, or

⁷By contrast, in case C label N can take only two values — 0 and 1.

rightwards in the columns, correspondingly. The numbers $S_{L,N=0}^{(a)} \equiv S_L^{(a)}$ were already listed in table (3.5).

It is helpful to look at the up-down diagonals in this table. The rightmost diagonal contains units only. the next one contains numbers $(L-1)$. For numbers staying in diagonals from third to seventh one finds expressions

$$\frac{(L-2)(L-3)\cdot(2L+1)}{2\cdot 3}, \quad (3.18)$$

$$\frac{(L-2)(L-3)(L-4)(L-5)\cdot(2L+1)(2L+3)}{2^2\cdot 3^2\cdot 5}, \quad (3.19)$$

$$\frac{(L-3)(L-4)^2(L-5)(L-6)(L-7)\cdot(2L-1)(2L+1)(2L+3)(2L+5)}{2^4\cdot 3^3\cdot 5^2\cdot 7}, \quad (3.20)$$

$$\frac{(L-3)(L-4)(L-5)^2(L-6)^2(L-7)(L-8)(L-9)\cdot(2L-1)(2L+1)^2(2L+3)(2L+5)(2L+7)}{2^6\cdot 3^4\cdot 5^3\cdot 7^2\cdot 9}, \quad (3.21)$$

$$\frac{(L-4)(L-5)^2(L-6)^2(L-7)^2(L-8)^2(L-9)(L-10)(L-11)\cdot(2L-3)(2L-1)(2L+1)^2(2L+3)^2(2L+5)(2L+7)(2L+9)}{2^9\cdot 3^5\cdot 5^4\cdot 7^3\cdot 9^2\cdot 11}. \quad (3.22)$$

With these data one can guess general formula for $S_{L,N}^{(a)}$.

Conjecture 4 (Case A: detailed distributions). Denote $n := [\frac{L-1}{2}] - N$. Integer n starts from 0 and labels leftwards the up-down diagonals in the table (3.17). One has

$$S_{L,N}^{(a)} = 2^{-[n^2/4]} \prod_{p=1}^n \frac{1}{(2p-1)!!} \prod_{p=0}^{[\frac{n-1}{3}]} \frac{(L - [\frac{n+p}{2}] - p - 1)!}{(L - 2n + 3p)!} \prod_{p=0}^{[\frac{n-2}{3}]} \frac{(2L + 2n - 6p - 3)!!}{(2L - 2[\frac{n+p}{2}] + 4p + 1)!!} \quad (3.23)$$

The same sequence was guessed recently in [13]⁸. Our notation is related to that used in [13] as $S_{L,N=[(L-1)/2]-n}^{(a)} \equiv R(n+1, L+1)$ (see eq.(17) there).

As it is explained, e.g., in [11, 13] the numbers given by formula (3.23) appear in counting elements of certain families of vertically symmetric alternating sign matrices. It is not however clear how one can characterize these families of ASMs. The table (3.17) suggests another combinatorial interpretation of integers $S_{L,N}^{(a)}$.

Pascal's hexagon relations. The numbers in sequence $S_{L,N}^{(a)}$ (3.23) satisfy equalities

$$S_{L-1,N}^{(a)} S_{L+1,N+1}^{(a)} + S_{L,N-1}^{(a)} S_{L,N+1}^{(a)} = S_{L-1,N+1}^{(a)} S_{L+1,N}^{(a)}, \quad \text{if } L \text{ is even,} \quad (3.24)$$

$$S_{L-1,N}^{(a)} S_{L+1,N+1}^{(a)} + S_{L,N}^{(a)} S_{L,N+2}^{(a)} = S_{L-1,N+1}^{(a)} S_{L+1,N}^{(a)}, \quad \text{if } L \text{ is odd.} \quad (3.25)$$

⁸For a particular case $L = 2p$, $N = 1$ distributions $S_{2p,1}^{(a)}$ coincide with $P_p(1)$, where $P_p(k)$ is the unnormalized probability to have k clusters in the stationary state (see [12]). An expression for $P_p(k)$ is given in Conjecture 3 in [11].



Figure 4: In case A configurations a)/b) of a size $L = 9/10$ have no 0- and 1-contacts. Thus, they belong to subset $\{w\}_{Dyck}^{N=2}$. In this subset among all the configurations of a fixed size $L = 9/10$ they have maximal possible number $n = 2$ of 2-contacts and in accordance with the statement of Conjecture 5 they enter the stationary state with a maximal coefficients $M_{L=9/10, N=2}^{(a)}$.

Substituting label N by $n := ([\frac{L-1}{2}] - N)$ in the notation $S_{L,N}^{(a)}$ one can uniformly write relations (3.24), (3.25) as

$$S_{L-1,n}^{(a)} S_{L+1,n}^{(a)} + S_{L,n-1}^{(a)} S_{L,n+1}^{(a)} = S_{L-1,n-1}^{(a)} S_{L+1,n+1}^{(a)}. \quad (3.26)$$

In table (3.17) numbers participating in eq.(3.26) form a hexagonal structure. One such hexagon is drawn in the table. The components of each square monomial in (3.26) occupy opposite vertices of the hexagon. Relation (3.26) thus looks as a sophisticated variant of the Pascal's triangle relation, wherefrom our notation follows.

Like in the Pascal's triangle case relations (3.26) can be used to reconstruct all numbers $S_{L,n}^{(a)}$ provided some, say boundary, part of them are fixed. For certain boundary data the numbers $S_{L,n}^{(a)}$ turn out to be integers and one recognizes among them the numbers of vertically symmetric and half turn symmetric alternating sign matrices, A_{2n+1}^V and A_n^{HT} , whereas the total number of ASMs A_n , and the number of vertically and horizontally symmetric ASMs A_n^{VH} appear in combinations. A brief discussion of this subject is presented in the Appendix.

We finish the section with observations of detailed maxima and of symmetry properties of the stationary distribution.

Conjecture 5 (Case A: detailed maxima). *In the stationary state of the case A RPM maximal coefficient $M_{L,N}^{(a)}$ in the subset $\{w\}_{Dyck}^N$ stands for configuration with a maximal possible number $([(L-1)/2] - N)$ of N -contacts (see explanations on Fig.(4)). It is given by formula*

$$M_{L,N}^{(a)} = S_{L-1,N-\epsilon(L)}^{(a)}, \quad (3.27)$$

where $\epsilon(L) := \frac{1-(-1)^L}{2}$ is a parity function.⁹

The relation (3.27) was also observed in [13]. Note that in case $N = 0$ and L odd we use in eq.(3.27) an extension of sequence $S_{L,N}^{(a)}$ to case $N = -1$ that we made in table (3.17).

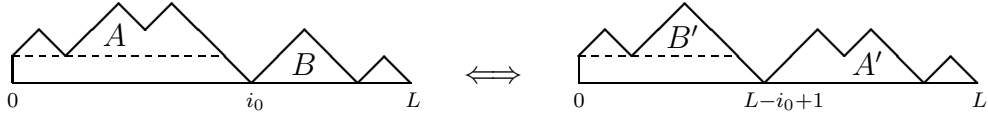
⁹Here and everywhere below in the main text we use definition of $S_{L,N}^{(a)}$ as it is given in eq.(3.23). This notation is natural for the stochastic models we are treating. Different convention about the second index in $S_{L,n}^{(a)}$ is used in eq.(3.26) and in the Appendix. It is more suitable from a mathematical viewpoint.

Note also that equality $M_{L=2p+1, N=0}^{(a)} = M_{L=2p+1, N=1}^{(a)}$ following from (3.27) agrees with the statements made in Conjecture 3 (see Fig.(3), picture d), cases $k=1$ and $k=L$).

Conjecture 6. *In the case A RPM for any configuration $\{h_i\}$ there exists a configuration $\{h'_i\}$ which appears in the stationary state with the same coefficient. The definition of $\{h'_i\}$ is following*

- for L even, $h'_i := h_{L-i}$;
- for L odd, let i_0 be coordinate of the leftmost 0-contact point in configuration $\{h_i\}$, or $i_0 = L$ if there is no 0-contacts in $\{h_i\}$. Then, $h'_i := h_{L-i} + 1$ for all $i \leq L - i_0$, and $h'_i := h_{L-i} - 1$ for all $i > L - i_0$.

For L even the statement of Conjecture 6 is a direct consequence of the left-right symmetry of the Hamiltonian and the configuration space. For L odd the space of the states is no more left-right symmetric, and the symmetry is not an obvious one. Typical pair of symmetric configurations is drawn below (pieces of paths A/B and A'/B' are left-right symmetric).



3.4 Case B: left orbits and factorizations to case A

Again, we start with a few definitions.

Consider a configuration $w = \{h_k\}_{k=0, \dots, L}$ from the set of Anchored Cross paths. For any N -contact point i of the configuration w we construct new configurations $w_l(i)$ and $w_r(i)$ (here value of N is irrelevant)

$$w_l(i) = \{h'_k\} : \quad h'_k := \begin{cases} h_k + 2 & \text{for } 0 \leq k \leq i, \\ h_k & \text{for } i < k \leq L, \end{cases} \quad (3.28)$$

$$w_r(i) = \{h''_k\} : \quad h''_k := \begin{cases} h_k & \text{for } 0 \leq k < i, \\ h_k + 2 & \text{for } i \leq k \leq L, \end{cases} \quad (3.29)$$

It may happen that either one or both configurations $w_l(i)$ and $w_r(i)$ defined by eqs.(3.28), (3.29) do not satisfy condition c) of the definition (2.10) of Anchored Cross paths. Such configurations $w_l(i)/w_r(i)$ should undergo total avalanche (see the end of Sec. 3.1), i.e., they are to be redefined as

$$\{h'_k\}_{k=0, \dots, L} \longrightarrow \{h''_k\}_{k=0, \dots, L}, \quad (3.30)$$

Thus defined configurations $w_l(i)$ and $w_r(i)$ are called, respectively, *left and right coverings of the configuration w at the point i* . Below, using the notion of left and right coverings we give an iterative description of left and right orbits of the configuration w .

Let $L(w, N)/R(w, N)$ denote a set of all N -contacts of w which do not occupy right/left boundary point and which are placed to the left/right of any k -contact with $k < N$. First, we

construct left/right coverings $w_l(i)/w_r(j)$ of w at all points $i \in L(w, N)/j \in R(w, N)$. Note that for all coverings $w_l(i)/w_r(j)$ the sets $L(w_l(i), N)/R(w_r(j), N)$ lie strictly inside the set $L(w, N)/R(w, N)$. Next, we construct left/right coverings for all obtained at a first step configurations $w_l(i)/w_r(j)$ at all points from their corresponding sets $L(w_l(i), N)/R(w_r(j), N)$. We repeat the procedure until at some step of iteration there will be no more N -contacts available for generation of new coverings. The set of all thus obtained left/right coverings together with w itself is called *left/right N-orbit of the configuration w* and is denoted as $\mathcal{O}_l(w, N)/\mathcal{O}_r(w, N)$; w is called *generating element* of the orbit. The process of iterative construction of left and right orbits is illustrated on Fig.6, p.30 and Fig.7, p.31, respectively. One can see that the numbers of elements in the orbits $\mathcal{O}_l(w, N)/\mathcal{O}_r(w, N)$ and in the sets $L(w, N)/R(w, N)$ are related as

$$\#\mathcal{O}_l(w, N) = 2^{\#L(w, N)}, \quad \#\mathcal{O}_r(w, N) = 2^{\#R(w, N)}. \quad (3.31)$$

An N -orbit is called *maximal* if it is not a subset of some bigger N -orbit.

For the family of Ballot paths only the procedure of left covering makes sense and, hence, only the left orbits are defined. In the rest of this section we apply notion of the left orbits to establish detailed relations for the stationary states in case B raise and peel model. The maximal 0- and 1-orbits will be especially important for us. The reasons are following.

The family of Ballot paths splits uniquely into collection of all (mutually nonintersecting) maximal left 0-/1-orbits.

The maximal left 0-orbits of length L are generated by elements

$$w = \{h_k\}_{k=0, \dots, L} : \quad h_0 = \begin{cases} 0 & \text{for } L \text{ even,} \\ 1 & \text{for } L \text{ odd.} \end{cases} \quad (3.32)$$

The maximal left 1-orbits of length L are generated by elements

$$w = \{h_k\}_{k=0, \dots, L} : \quad h_0 = \begin{cases} \text{either 0, or 2} & \text{for } L \text{ even,} \\ 1 & \text{for } L \text{ odd.} \end{cases} \quad (3.33)$$

We further observe that sums of the stationary coefficients over maximal left 0- and 1-orbits in case B are related to certain stationary coefficients in case A. These relations generalizing formula (3.7) are presented in

Conjecture 7. *Take any Dyck paths u and v of the lengths L and $(L + 1)$, respectively. Denote *v a Ballot path of the length L which is a (left) reduction of the Dyck path v , i.e.,*

$$h_k({}^*v) = h_{k+1}(v), \quad \text{for all } k = 0, \dots, L.$$

With these notations one has

$$\text{for } L \text{ even: } \sum_{\nu \in \mathcal{O}_l(u, 0)} p_L^{(b)}(\nu) = S_{L+1}^{(a)} p_L^{(a)}(u), \quad \sum_{\nu \in \mathcal{O}_l({}^*v, 1)} p_L^{(b)}(\nu) = S_L^{(a)} p_{L+1}^{(a)}(v), \quad (3.34)$$

$$\text{for } L \text{ odd: } \sum_{\nu \in \mathcal{O}_l(*v,0)} p_L^{(b)}(\nu) = S_L^{(a)} p_{L+1}^{(a)}(v), \quad \sum_{\nu \in \mathcal{O}_l(u,1)} p_L^{(b)}(\nu) = S_{L+1}^{(a)} p_L^{(a)}(u). \quad (3.35)$$

Here summation is taken over all elements of the left 0-, or 1-orbits generated by u , or $*v$ (note that configurations u and $*v$ span all generating elements described in (3.32), (3.33)).

Combining the last conjecture with conjectures 4–6 from the previous section one can get explicit values for sums over certain 0- and 1-orbits. These results and similar formulas for higher orbits are presented in the next

Conjecture 8. *Let us denote $W(h_0, s) = \{h_k\}_{k=0, \dots, L}$ a Ballot path of a size L such that for a given left boundary height h_0 it has maximal possible number of s -contact points. We are interested in configurations where s take values between $\max\{0, (h_0 - 1)\}$ and $(\frac{L+h_0}{2} - 1)$ (see Fig.(5)).*

One can guess explicit expressions for sums of the coefficients $p_L^{(b)}$ over left h_0 - and $(h_0 - 1)$ -orbits generated by elements $W(h_0, s)$. For even size L parameter h_0 takes on even values from 0 to L and one has relations

$$\begin{aligned} (h_0 = 2m)\text{-orbits:} \quad & \sum_{\nu \in \mathcal{O}_l(W(h_0=2m,s),2m)} p_L^{(b)}(\nu) = S_{L+1,m}^{(a)} S_{L-1,s-m}^{(a)}, \\ (h_0 - 1 = 2m - 1)\text{-orbits:} \quad & \sum_{\nu \in \mathcal{O}_l(W(h_0=2m,s),2m-1)} p_L^{(b)}(\nu) = S_{L,m-1}^{(a)} S_{L,s-m}^{(a)}. \end{aligned} \quad (3.36)$$

The last formula is applicable in case $m = 0$, i.e., for (-1) -orbits. In this case all the (-1) -orbits are treated as singlets containing their generating elements only.

For odd size L parameter h_0 takes on odd values from 1 to L and one has relations

$$\begin{aligned} (h_0 - 1 = 2m)\text{-orbits:} \quad & \sum_{\nu \in \mathcal{O}_l(W(h_0=2m+1,s),2m)} p_L^{(b)}(\nu) = S_{L,m}^{(a)} S_{L,s-m}^{(a)}, \\ (h_0 = 2m + 1)\text{-orbits:} \quad & \sum_{\nu \in \mathcal{O}_l(W(h_0=2m+1,s),2m+1)} p_L^{(b)}(\nu) = S_{L+1,m}^{(a)} S_{L-1,s-m-1}^{(a)}. \end{aligned} \quad (3.37)$$

This Conjecture is graphically illustrated on Fig.6 on page 30.

Most of the orbits appearing in the left hand sides of relations (3.36) and (3.37) are singlets and doublets. Namely, one has singlet $(h_0 - 1)$ -orbits in case $s \geq h_0$ and singlet h_0 -orbits for $s = h_0 - 1$; one has doublet h_0 -orbits in case $s \geq h_0 + 1$. The larger size $2\frac{L-h_0}{2}$ -plet h_0 - and $(h_0 - 1)$ -orbits appear, respectively, for $s = h_0$ and $s = h_0 - 1$.

Relations for singlets and doublets provide explicit expressions for a number of stationary state coefficients in case B RPM. In particular, formulas for $(h_0 - 1)$ -singlets generated by elements $W(h_0, s)$ with $s \geq h_0$ were observed in [13].

Noticing that two configurations from h_0 -doublet generated by $W(h_0, h_0 + 1)$ correspond to $(h_0 - 1)$ - and $(h_0 + 2)$ -singlets generated by $W(h_0, h_0 + 1)$ and $W(h_0 + 2, h_0 + 1)$, respectively,

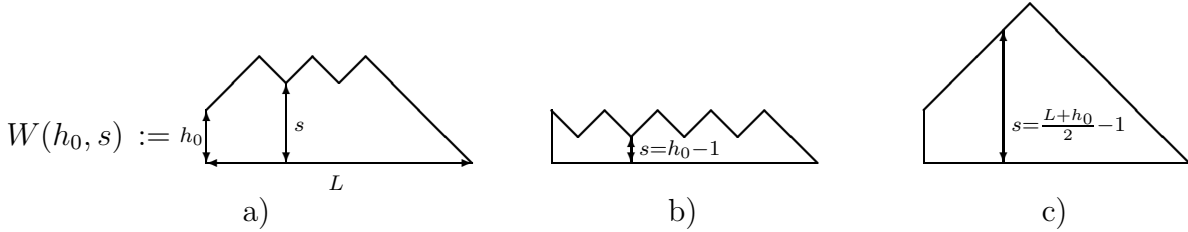


Figure 5: A typical configuration $W(h_0, s)$ is shown on picture a). It is uniquely defined by its size L , its left boundary height h_0 and the height s of its contact points in the bulk. A number of s -contacts in such configuration equals $(\frac{L+h_0}{2} - s - 1)$. Boundary cases with $s = (h_0 - 1)$ and $s = (\frac{L+h_0}{2} - 1)$ are shown, respectively, on pictures b) and c). In the last case one uses parameter s just by analogy, because configuration c) contains 0 number of contacts in the bulk.

one concludes that expressions from the right hand sides of relations (3.36) and (3.37) should comply certain consistency rules. These are just the Pascal's hexagon relations (3.24), (3.25) and in this way the Pascal's hexagon relations were first time observed.

We finish the section with several observations about detailed normalizations and extrema in case B.

Conjecture 9 (Case B: detailed distributions I). *For the quantities $S_{L,N}^{(b)}$ introduced in (3.16) one has formulas*

$$\begin{aligned} \text{for } L \text{ even: } S_{L,N}^{(b)} &= S_{L+1,[\frac{N+1}{2}]}^{(a)} S_{L,[\frac{N}{2}]}^{(a)}, \\ \text{for } L \text{ odd: } S_{L,N}^{(b)} &= S_{L+1,[\frac{N}{2}]}^{(a)} S_{L,[\frac{N+1}{2}]}^{(a)}. \end{aligned} \quad (3.38)$$

The same formulas for $S_{L,N}^{(b)}$ were observed in [13] (see eq.(48) there).

We remind that label N refers to global minimum of Ballot paths contributing to distribution $S_{L,N}^{(b)}$ (it should be greater or equal to N). N may take all integer values from 0 to L . For $N = 0$ relations (3.38) coincide with eq.(3.7).

One can consider another set of detailed distributions $\Sigma_{L,N,M}^{(b)}$ which count stationary state contributions of all configurations w whose left boundary height is fixed as $h_0(w) = N$ and whose all s -contacts in the bulk satisfy condition $s \geq M$ (i.e., whose global minimum in the bulk is greater or equal to M). For $M \geq N$ all such configurations can be obtained by adding tiles (not half-tiles!) to the configuration $W(h_0 = N, s = M)$ drawn on Fig.5 a).

Note that by contrast with the previous case label N in the notation $\Sigma_{L,N,M}^{(b)}$ may take only integers between zero and L which are of the same parity as L .

Conjecture 10 (Case B: detailed distributions II). *In case $M \geq N$ quantities $\Sigma_{L,N,M}^{(b)}$ are given by formula*

$$\Sigma_{L,N,M}^{(b)} = S_{L+1, M - [\frac{N-1}{2}]}^{(a)} S_{L, [\frac{N-1}{2}]}^{(a)}. \quad (3.39)$$

We were unable to find similar expressions in case $M < N$.

The right hand sides of eqs.(3.38) and (3.39) contain the same square combination $S_{L+1,X}^{(a)} S_{L,Y}^{(a)}$ but for indices X, Y taking values in adjacent domains. Hence, formally speaking one can view distributions $S_{L,N-1}^{(b)}$ and $S_{L,N-2}^{(b)}$ as extrapolations of distribution $\Sigma_{L,N,M}^{(b)}$ to cases $M = N - 1$ and $M = N - 2$, respectively. However, we don't know any non-formal explanation to this fact.

Conjecture 11 (Case B: detailed extremes). *Among elements of the set $\{w\}_{\text{Ballot}}^N$ configuration with maximal possible number $[\frac{L-N}{2}]$ of N -contacts enters the stationary state with the maximal coefficient $M_{L,N}^{(b)}$ (see def.(3.16)). All such configurations are generating elements $W(h_0, s = h_0 - 1)$, or $W(h_0, s = h_0)$, respectively, for h_0 -, or $(h_0 - 1)$ -singlet orbits. Hence, expressions for maxima $M_{L,N}^{(b)}$ are particular cases of formulas (3.36), (3.37) (index s there corresponds to N in the notation for detailed maxima). They are*

$$\begin{aligned} \text{for } L \text{ even:} \quad M_{L,N=2m}^{(b)} &= S_{L,m-1}^{(a)} S_{L,m}^{(a)}, \\ M_{L,N=2m+1}^{(b)} &= S_{L+1,m+1}^{(a)} S_{L-1,m}^{(a)}; \end{aligned} \quad (3.40)$$

$$\begin{aligned} \text{for } L \text{ odd:} \quad M_{L,N=2m}^{(b)} &= S_{L+1,m}^{(a)} S_{L-1,m-1}^{(a)}, \\ M_{L,N=2m+1}^{(b)} &= S_{L,m}^{(a)} S_{L,m+1}^{(a)}. \end{aligned} \quad (3.41)$$

In case of L even and $N = 0$ there is one more configuration $w = \{h_0 = 2, h_i = \epsilon(i)\}$ (see Fig.3 b) on p.10) which enters the stationary state with the same maximal coefficient.

Among all Ballot paths with the same left boundary height h_0 configuration which have no any contact points in the bulk enters the stationary state with a minimal coefficient $m_{L,h_0}^{(b)}$. All such configurations are generating elements $W(h_0, s = \frac{L+h_0}{2} - 1)$ of $(h_0 - 1)$ -singlet orbits. So, expressions for $m_{L,h_0}^{(b)}$ can be found among formulas eqs.(3.36), (3.37). They are

$$m_{L,h_0}^{(b)} = S_{L, [\frac{h_0-1}{2}]}^{(a)}. \quad (3.42)$$

3.5 Case C: right orbits and factorizations to case B

In this section we consider right 0- and 1-orbits in a family of Anchored Cross paths and describe corresponding stationary distributions for the case C raise and peel model. Our key observations are following.

The family of Anchored Cross paths splits uniquely into collection of all (mutually non-intersecting) maximal right 0/1-orbits.

The maximal right 0-orbits of length L are generated by elements

$$w = \{h_k\}_{k=0,\dots,L} : \quad h_L = 0. \quad (3.43)$$

The maximal right 1-orbits of length L are generated by elements

$$w = \{h_k\}_{k=0,\dots,L} : \quad \text{either } h_L = 0, \text{ or } h_L = 2 \text{ and } \min_{0 \leq i \leq L} h_i = 1 \text{ (i.e., } \neq 0\text{).} \quad (3.44)$$

We further observe that sums of the stationary coefficients over maximal right 0- and 1-orbits in case C are related to certain stationary coefficients in case B. These relations generalizing formula (3.8) are given in

Conjecture 12. *Take any Ballot paths u and v of the lengths L and $(L+1)$, respectively. Denote v^* an Anchored Cross path of the length L which is a (right) reduction of the Ballot path v , i.e.,*

$$\text{for all } k = 0, \dots, L, \quad h_k(v^*) = \begin{cases} h_k(v) + 1, & \text{if } \min_{k=0}^L h_k(v) = 0, \\ h_k(v) - 1, & \text{otherwise.} \end{cases}$$

With these notations one has

$$\sum_{\nu \in \mathcal{O}_r(u,0)} p_L^{(c)}(\nu) = \text{Denominator of } \left(\frac{S_L^{(a)}}{S_{L+2}^{(a)}} \right) p_L^{(b)}(u) \equiv \frac{m_L^{(c)} S_{L+2}^{(a)}}{S_L^{(a)}} p_L^{(b)}(u), \quad (3.45)$$

$$\sum_{\nu \in \mathcal{O}_r(v^*,1)} p_L^{(c)}(\nu) = \text{Numerator of } \left(\frac{S_L^{(a)}}{S_{L+2}^{(a)}} \right) p_{L+1}^{(b)}(v) \equiv m_L^{(c)} p_{L+1}^{(b)}(v). \quad (3.46)$$

Here summation is taken over all elements of the right 0-, or 1-orbits generated by u , or v^* (configurations u and v^* span all generating elements described in (3.43), (3.44)).

This Conjecture is graphically illustrated on Fig.7 on page 31.

Remark 1. In normalization (3.12) relations (3.45) and (3.46) read

$$\sum_{\nu \in \mathcal{O}_r(u,0)} \tilde{p}_L^{(c)}(\nu) = S_{L+2}^{(a)} p_L^{(b)}(u), \quad (3.47)$$

$$\sum_{\nu \in \mathcal{O}_r(v^*,1)} \tilde{p}_L^{(c)}(\nu) = S_L^{(a)} p_{L+1}^{(b)}(v). \quad (3.48)$$

In this presentation Conjecture 12 looks very much in the spirit of Conjecture 7 and one can be immediately convinced that it refines formula (3.13).

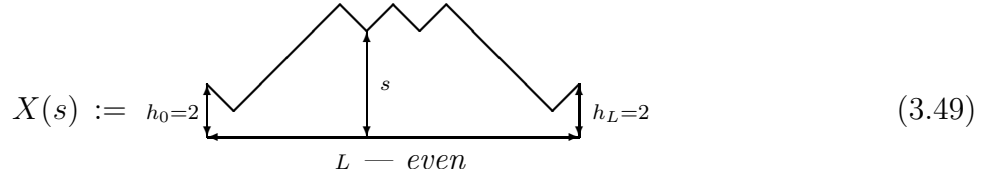
Remark 2. The case C RPM stationary state obeys mirror symmetry. Namely, any pair of configurations $\{h_k\}$ and $\{h'_k\}$ whose shapes are left-right symmetric, i.e.,

$h'_k = h_{L-k}$ for all k in case of L even;

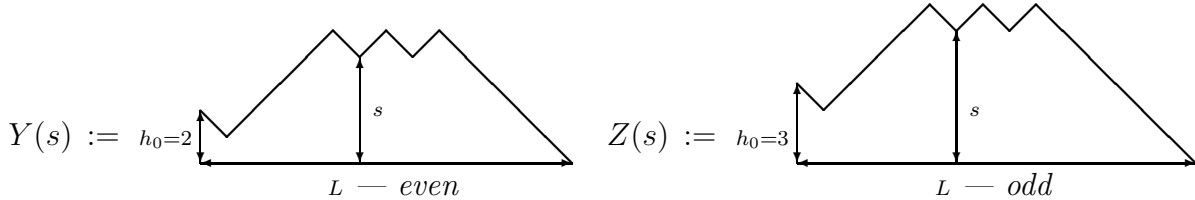
$$h'_k = \begin{cases} h_{L-k} + 1, & \text{if } \min_{i=0}^L h_i = 0, \\ h_{L-k} - 1, & \text{if } \min_{i=0}^L h_i = 1, \end{cases} \quad \text{for all } k \text{ in case of } L \text{ odd;}$$

enter the stationary state with the same coefficients. Using this symmetry one can reformulate Conjecture 12 in the language of left orbits.

There are many singlets and doublets among the orbits appearing in the right hand sides of eqs.(3.45) and (3.46). E.g., all 0-orbits generated by elements $w : h_L(w) = 0$ and $h_k(w) \geq 1 \forall k = 1, \dots, L-1$, are doublets; all 1-orbits generated by configurations $w : h_L(w) = 0$ are singlets. Relations for singlets and doublets provide a number of explicit expressions for stationary state coefficients in the case C RPM. In particular, expressions which are presented in a right column of Table 2 in [13] all correspond to the right 1-singlets. To illustrate the practical use of Conjectures 12 and 8 we shall derive here formulas for stationary state coefficients of configurations



where configuration's size L may take even values only and parameter s runs from 1 to $\frac{(L-2)}{2}$. Denote



According to Conjectures 8 and 12 the stationary state coefficients for these configurations and for configurations $W(h_0 = 0, s)$ and $W(h_0 = 1, s)$ (see fig.5 on p.17) satisfy relations

$$\text{right 0-doublet (eq.(3.45))}: \quad p_L^{(c)}(Y(s)) + p_L^{(c)}(X(s)) = \frac{m_L^{(c)} S_{L+2}^{(a)}}{S_L^{(a)}} p_L^{(b)}(Y(s)), \quad (s \geq 1),$$

$$\text{right 1-singlet (eq.(3.46))}: \quad p_L^{(c)}(Y(s)) = m_L^{(c)} p_{L+1}^{(b)}(Z(s+1)),$$

$$\text{left 0-doublet (first eq.(3.36))}: \quad p_L^{(b)}(W(0, s)) + p_L^{(b)}(Y(s)) = S_{L+1}^{(a)} S_{L-1,s}^{(a)}, \quad (s \geq 1),$$

$$\text{left } (-1)\text{-singlet (second eq.(3.36))}: \quad p_L^{(b)}(W(0, s)) = S_L^{(a)} S_{L,s}^{(a)},$$

$$\text{left 1-doublet (second eq.(3.37))}: \quad p_{L+1}^{(b)}(W(1, s+1)) + p_{L+1}^{(b)}(Z(s+1)) = S_{L+2}^{(a)} S_{L,s}^{(a)}, \quad (s \geq 1),$$

$$\text{left 0-singlet (first eq.(3.37))}: \quad p_{L+1}^{(b)}(W(1, s+1)) = S_{L+1}^{(a)} S_{L+1,s+1}^{(a)},$$

wherefrom one obtains

$$p_L^{(c)}(X(s)) = m_L^{(c)} \left\{ \frac{S_{L+2}^{(a)} S_{L+1}^{(a)} S_{L-1,s}^{(a)}}{S_L^{(a)}} - 2 S_{L+2}^{(a)} S_{L,s}^{(a)} + S_{L+1}^{(a)} S_{L+1,s+1}^{(a)} \right\}. \quad (3.50)$$

In the last conjecture we describe maximal components of the stationary states in the case C RPM.

Conjecture 13 (Case C: maxima). *The maximal coefficient $M_L^{(c)}$ appear in the set $\{p_L^{(c)}\}$ with multiplicity 1 for L even and 2 for L odd.*

For L odd one of the corresponding interface configurations is the substrate shown on Figure 3 c) on page 10. The second one is a mirror image of the first (see Remark 2 to Conjecture 12). For L even the corresponding configuration is $X(1)$ (see def.(3.49)). Explicit values of the maximal coefficients are

$$\text{for } L \text{ odd: } M_L^{(c)} = m_L^{(c)} S_L^{(a)} S_{L+2,1}^{(a)}, \quad (3.51)$$

$$\text{for } L \text{ even: } M_L^{(c)} = m_L^{(c)} \left\{ \frac{S_{L+2}^{(a)} S_{L-1}^{(a)} S_{L+1,1}^{(a)}}{S_L^{(a)}} - S_L^{(a)} S_{L+2,1}^{(a)} \right\}. \quad (3.52)$$

Relation (3.52) is a particular case of eq.(3.50) simplified with the use of Pascal's hexagon relations.

A mirror image of the configuration $X(1)$, which is the substrate, enters the stationary state with next to leading coefficient

$$\text{for } L \text{ even: } p_L^{(c)}(\text{Substrate}) = m_L^{(c)} S_{L+1}^{(a)} S_{L+1,1}^{(a)}. \quad (3.53)$$

4 Discussion

Two of the issues discussed in this paper are most interesting from author's point of view and deserve further investigation.

The first one is the Pascal's hexagon relation which surprisingly comes as defining recurrent equation for some of the RPM's stationary coefficients. At the moment we do not have explanation for this fact. A very preliminary investigation of the Pascal's hexagon relation was carried out in the Appendix. It comes out that besides the solution $S_{L,N}^{(a)}$ (3.23) which is related to RPM with open boundaries the relation admits also solutions which manifest themselves in the periodic stochastic models (see eq.(A.8) and the sentence above it; see also remark 4 on page 24) and that it is related also to ASM combinatorics (see eqs.(A.27)–(A.38)). As author has learned from Yuri Stroganov the Pascal's hexagon relations are similar to bilinear equations, like octahedron recurrence, number walls, S-arrays which are actively discussed in algebraic combinatorics community (see, e.g., bilinear forum on the web). Moreover it has already appeared once in a physical literature as certain 2-dimensional reduction of the Hirota difference equation, called the discrete Boussinesq equation (see eq.(8.11) in [25] and the references therein).

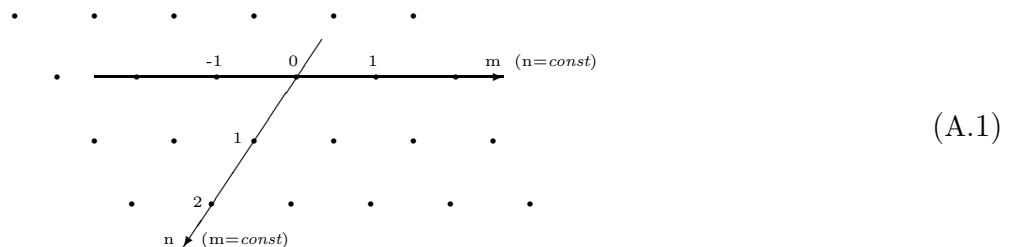
The second one is the notion of orbits which appears while investigating the case B and case C RPMs and which is responsible for interrelations of the stationary state coefficients in cases A, B and C. The similar relations also appear for the spectra of these models [14]. This facts suggest an idea that cases B and A RPMs can be subsequently obtained by factorization of the case C. It would be interesting to find such conjectural factorization at the level of boundary extended Temperley-Lieb algebras.

5 Acknowledgements

The author is grateful to Jan de Gier, Andrey Mudrov, Bernard Nienhuis, Yuri Stroganov and Nikolai Tyurin for useful discussions. Special thanks to Vladimir Rittenberg whose constant interest in the subject and valuable advices provide a lot of inspiration to this work. The work is supported in part by RFBR grant # 03-01-00781 and by the grant of Heisenberg-Landau Foundation. The author gratefully acknowledges warm hospitality of Physikalisches Institut of the University of Bonn and of Lorentz Center at the University of Leiden where this work was completed.

Appendix. Solutions of Pascal's hexagon relation and ASM numbers

Consider a set of numbers which are placed on vertices of a planar trigonal lattice. Introducing coordinate lines on the lattice as it is shown on figure (A.1) we label the numbers in the set by a pair of integers: $\{f_{m,n}\}$, $m, n \in \mathbb{Z}$.



For any six numbers a, a', b, b', c, c' in the set which are situated on apices of a hexagon



we impose a condition

$$aa' + bb' = cc', \quad (A.3)$$

which can be viewed as a generalization of Pascal's triangle relation to the case of hexagon. In coordinatization (A.1) it reads

$$f_{m-1,n} f_{m+1,n} + f_{m,n-1} f_{m,n+1} = f_{m-1,n-1} f_{m+1,n+1}. \quad (\text{A.4})$$

A particular solution of the Pascal's hexagon relation is given by formulas

$$f_{m,n} = 2^{-[n^2/4]} \prod_{p=1}^n \frac{1}{(2p-1)!!} \prod_{p=0}^{[\frac{n-1}{3}]} \frac{(m - [\frac{n+p}{2}] - p - 1)!}{(m - 2n + 3p)!} \prod_{p=0}^{[\frac{n-2}{3}]} \frac{(2m + 2n - 6p - 3)!!}{(2m - 2[\frac{n+p}{2}] + 4p + 1)!!}, \quad (\text{A.5})$$

$$f_{-m,-n} = 2^{-[n^2/4]} \prod_{p=1}^{n-1} \frac{1}{(2p-1)!!} \prod_{p=0}^{[\frac{n}{3}-1]} \frac{(m - [\frac{n+p}{2}] - p - 2)!}{(m - 2n + 3p + 2)!} \prod_{p=0}^{[\frac{n-2}{3}]} \frac{(2m + 2n - 6p - 5)!!}{(2m - 2[\frac{n+p}{2}] + 4p - 1)!!}, \quad (\text{A.6})$$

where m is an integer and n is a nonnegative integer. Here for negative values of m ratios of factorials are treated as Pochhammer symbols:

$$(n-1)!/(k-1)! = \prod_{j=k}^{n-1} j =: (k)_{(n-k)}, \quad (2n-1)!!/(2k-1)!! = 2^{(n-k)} (k)_{(n-k)} (2k)_{(2n-2k)}. \quad (\text{A.7})$$

The corresponding distribution of numbers on the lattice is shown in table 1 on page 32.

Formulas (A.5) and (A.6) can be reproduced in a following way. First, one assigns certain initial data to $f_{m,n}$ (like in the Pascal's triangle case)

$$f_{m \geq 0, n=0} = 1, \quad f_{m \geq 0, n=-1} = 1, \quad f_{m=2n-1, n>0} = 0, \quad (\text{A.7})$$

and calculates values of $f_{m,n}$ for $n > 0$ and $m \geq 2n$ row by row (i.e., consecutively for $n = 1, 2, 3$, etc.) using relations (A.4). In this way formula (A.5) for detailed distributions $S_{L,n}^{(a)} = f_{m=L,n}$ was obtained in Sec. 3.3.

Then, one observes that formula (A.5) is well defined on a half-plane $n \geq 0$ and gives numbers satisfying Pascal's hexagon relation in this sector. Note that combinatorial functions $R(n, L)$ and $Q(n, L)$ introduced in [13] (see eqs.(16) and (17) there) both are related to function (A.5)

$$f_{m,n} = R(n+1, m+1), \quad f_{-m,n} = (-1)^{[\frac{n+1}{2}]} Q(n+1, m+n+1). \quad (\text{A.8})$$

Note also that in the sector $m \leq 2n-1$, $n \leq 2m-1$ numbers $f_{m,n}$ vanish (see tab.(1)) that, in particular, destroys the connection between numbers $f_{m,n}$ in sectors $m \geq 2n$, $n \geq 0$ and $2m \leq n$, $n \geq 0$ via the Pascal's hexagon relations.

Further on, comparing numbers $f_{m,n}$ in sectors $m \geq 2n \geq 0$ and $n \geq 2m \geq 0$ one observes $m \leftrightarrow n$ symmetry

$$f_{m,n} = (-1)^{(mn + [4(m+n)/3])} 2^{-[(m-2n)/3]} f_{n,m} \quad \forall m \geq n \geq 0. \quad (\text{A.9})$$

Extrapolating this symmetry relation one defines numbers $f_{m,n}$ in sector $m \geq 0 \geq n$ through those from sector $n \geq 0 \geq m$. The Pascal's hexagon relation for the newly defined numbers stays valid.

Finally, one can guess general formula (A.6) for $f_{m,n}$ on a half-plane $n < 0$ analyzing the numbers in sector $m \geq 0 \geq n$. The numbers $f_{m,n}$ thus obtained satisfy relation (A.4) on the whole lattice. Let us end up discussion of the solution (A.5), (A.6) with a list of remarks/observations.

1. $f_{m,n}$ take particularly simple values along the following directions (see tab.1)

$$f_{m,0} = f_{m,-1} = 1 \quad (\text{A.10})$$

$$f_{0,n} = (-1)^{[4n/3]} 2^{[n/3]}, \quad f_{0,-n} = (-1/2)^{[2n/3]}, \quad \forall n \geq 0, \quad (\text{A.11})$$

$$f_{-1,n} = (-2)^{[(n+2)/3]}, \quad f_{-1,-n} = (-1)^{[(2-n)/3]} (1/2)^{[(2n-1)/3]}, \quad \forall n \geq 1, \quad (\text{A.12})$$

$$f_{m=2n-1,n>0} = f_{m>0,n=2m-1} = f_{m=2n+3,n<-2} = f_{m<-2,n=2m+3} = 0. \quad (\text{A.13})$$

Conditions (A.10)–(A.13) can be used as initial data for reconstruction of all the nonzero numbers $f_{m,n}$ by means of relation (A.4).

2. Symmetry relations (A.9) are valid for any pair m, n such that $m \geq n$ (but not for $m < n$).
3. The numbers $f_{m,n}$ given by eq.(A.5) are always integer. The numbers $f_{-m,-n}$ given by eq.(A.6) become integer upon multiplication by $2^{(n-1)}$.
4. The numbers $f_{m,n}$ in sectors $m \geq 2n \geq 0$ and $0 \leq n \leq 1 - m$ are known to be related to open and periodic one dimensional stochastic models, respectively (see [13] and Sec.3.3). One may expect that there exists some one dimensional stochastic process related to the numbers $f_{m,n}$ in sector $n \leq -1, m \leq 2n + 2$.

Next, we consider solutions of the Pascal's hexagon relation which are polynomials in one, or several variables. Evaluated at particular values of their variable(s) they produce numeric solutions to (A.4). We found two examples of polynomial solutions.

First one is a set of polynomials in two variables $F_{m,n}(x,y)$ which are defined in the sector $n \geq 0, m \geq 2n - 1$. They satisfy Pascal's hexagon relation (A.4) (just substitute $f_{m,n}$ by $F_{m,n}(x,y)$ there) and one can uniquely define them provided that polynomials on the boundaries of the sector are fixed. We choose

$$F_{m>0,0} = 1, \quad F_{m>1,1} = y + (m-2)x, \quad F_{m=2n-1,n>0} = 0, \quad (\text{A.14})$$

which is a generalization of boundary conditions (A.7). A nontrivial fact is that with such choice of the boundary conditions one obtains polynomial (rather than rational) expressions

for $F_{m,n}(x, y)$. In table 2 on page 33 some polynomials $F_{m,n}(x, y)$ for small values of m and n are listed.

The functions $F_{m,n}(x, y)$ obey rescaling symmetries¹⁰

$$F_{m,n}(x, y) = y^n F_{m,n}(x/y, 1), \quad \text{for } y \neq 0, \quad (\text{A.15})$$

$$F_{m,n}(x, 0) = x^n F_{m,n}(1, 0), \quad (\text{A.16})$$

$$F_{2n,n}(x, y) = y F_{2n,n-1}(x, y). \quad (\text{A.17})$$

It follows then that only two values $y = 0$ and $y = 1$ are essential. We keep using variable y as it is suitable for producing integral solutions to the Pascal's hexagon relations. In particular, one finds following relations between polynomials $F_{m,n}$ and the numbers given by formulas (A.5) and (A.6)

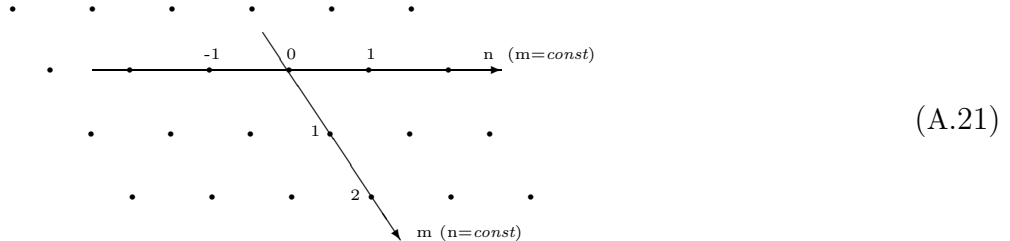
$$F_{m+1,n}(1, 0) = F_{m+2,n+1}(0, 1) = F_{m,n}(1, 1) = f_{m,n}, \quad (\text{A.18})$$

$$F_{m,n}(2, 3) = 2^n f_{-m,-n-1}. \quad (\text{A.19})$$

Another set of polynomials $G_{m,n}(x)$ are solutions of a variant of Pascal's hexagon relations

$$G_{m,n+1}G_{m,n-1} + G_{m+1,n-1}G_{m-1,n+1} = G_{m-1,n}G_{m+1,n}. \quad (\text{A.20})$$

These relations result from a different coordinatization of the Pascal's hexagon rules (A.2), (A.3). The coordinate frame for them looks as



¹⁰Rescaling properties (A.15), (A.16) are particular manifestations of “gauge” transformations on the set of solutions of Pascal's hexagon equation. Namely, once a solution $\{a, a', b, b', c, c'\}$ of eq.(A.3) is given a family of gauge equivalent solutions $\{\alpha a, \alpha' a', \beta b, \beta' b', \gamma c, \gamma' c'\}$ is parametrized by six scaling numbers $\alpha, \alpha', \beta, \beta', \gamma$ and γ' satisfying constraints $\alpha\alpha' = \beta\beta' = \gamma\gamma' \neq 0$. On a trigonal lattice this gauge transformation is uniquely defined provided one fixes 6 mutually independent scaling parameters for the vertices situated as shown on a figure

For this set of functions we impose boundary conditions

$$G_{0,n>0} = 1, \quad G_{1,n\geq 0} = 1 + nx, \quad G_{m>0,0} = x^{[(m+1)/3]}(x+1)^{[m/3]}(-1)^{[m/3]+[m/2]}, \quad (\text{A.22})$$

which allow one to iteratively reconstruct polynomials $G_{m,n}(x)$ (again, a nontrivial fact) in the sector $m \geq 0, n \geq 0$. In particular, one finds

$$G_{m,1} = x^{[m/3]}(x+1)^{[(m+2)/3]}(-1)^{[(m+2)/3]+[(m+1)/2]}. \quad (\text{A.23})$$

Boundary conditions (A.22), (A.23) are generalizations of the boundary data for $f_{m,n}$ along directions $m < 0, n \in \{0, 1\}$, and $n > 0, m \in \{0, -1\}$ (see table 1 and formulae (A.10)–(A.12)). Explicit expressions for $G_{m,n}(a)$ for small values of m and n are given in table 2 on page 33.

The functions $G_{m,n}(x)$ obey reflection symmetry

$$G_{m,n}(x) = x^{[(m-n+1)/3]} \tilde{x}^{-[(\tilde{m}-\tilde{n}+1)/3]} (-1)^{[(m+n)/2]} G_{\tilde{m},\tilde{n}}(\tilde{x}), \quad \text{for } x \neq 0, -1, \quad (\text{A.24})$$

$$G_{m,n}(0) = (-1)^{m+1} G_{m-1,n+1}(-1), \quad (\text{A.25})$$

where $\tilde{x} = -1 - x$, $\tilde{m} = n - 1$ and $\tilde{n} = m + 1$. At certain values of x they reproduce numbers (A.5)

$$G_{m,n}(0) = f_{m+n-1,m-1}, \quad G_{m,n}(1) = (-1)^{[(m+1)/2]} f_{-n,m}. \quad (\text{A.26})$$

Finally, it is remarkable that the solutions of the Pascal's hexagon relation reproduce in several ways numbers which were discovered in counting various symmetry classes of the alternating sign matrices (see [22, 23, 24]). Below we present list of such formulae. Relations (A.27), (A.28) and (A.31)–(A.34) were observed earlier in [13] (see eqs.(18)–(23) there). First equalities in (A.27) and (A.29) are particular manifestations of eq.(A.17).

$$\begin{aligned} F_{2n,n-1}(1,1) &= F_{2n,n}(1,1) = G_{n+1,n}(0) = G_{n,n+1}(0) \\ &= \{1, 3, 26, 646, \dots\} = A_{2n+1}^V, \quad n > 0, \end{aligned} \quad (\text{A.27})$$

$$F_{2n-1,n-1}(1,1) = G_{n,n}(0) = \{1, 1, 2, 11, 170, \dots\} = \frac{A_{4n\pm 1}^{VH}}{A_{2n\pm 1}^V}, \quad n \geq 0, \quad (\text{A.28})$$

$$F_{2n,n-1}(2,3) = \frac{1}{3} F_{2n,n}(2,3) = \{1, 7, 143, 8398, \dots\} = \frac{A_{2n-1}}{A_{2n-1}^V}, \quad n > 0, \quad (\text{A.29})$$

$$F_{2n+1,n}(2,3) = \{1, 5, 66, 2431, 252586, \dots\} = \frac{A_{4n}^{HT}}{A_{2n}} \frac{A_{2n\pm 1}^V}{A_{4n\pm 1}^{VH}}, \quad n \geq 0, \quad (\text{A.30})$$

$$G_{n,n}(1) = \{1, 2, 10, 140, 5544, \dots\} = A_{2n}^{HT}, \quad n \geq 0, \quad (\text{A.31})$$

$$G_{n,n+1}(1) = \{1, 3, 25, 588, 39204, \dots\} = A_{2n+1}^{HT}, \quad n \geq 0, \quad (\text{A.32})$$

$$G_{n+1,n}(1) = \{1, 2, 2 \times 7, 7 \times 42, 42 \times 429, \dots\} = A_n A_{n+1}, \quad n \geq 0, \quad (\text{A.33})$$

$$G_{n,n+2}(1) = \{1, 2^2, 7^2, 42^2, 429^2, \dots\} = (A_{n+1})^2, \quad n \geq 0, \quad (\text{A.34})$$

$$G_{n,n}(-\frac{1}{2}) = \{1, \frac{1}{2}, \frac{1}{2^2}, \frac{2^2}{2^3}, \frac{6^2}{2^4}, \frac{33^2}{2^5}, \frac{286^2}{2^6}, \dots\} = \frac{(A_{2n+1}^{VH})^2}{2^n}, \quad n \geq 0, \quad (\text{A.35})$$

$$G_{n+1,n}(-\frac{1}{2}) = \{1, \frac{1}{2}, \frac{2}{2^2}, \frac{2 \times 6}{2^3}, \frac{6 \times 33}{2^4}, \frac{33 \times 286}{2^5}, \dots\} = \frac{A_{2n+1}^{VH} A_{2n+3}^{VH}}{2^n}, \quad n \geq 0, \quad (\text{A.36})$$

$$G_{n,n+1}(-\frac{1}{2}) = \{1, 0, \frac{1}{2^2}, 0, \frac{3^4}{2^4}, 0, \frac{26^4}{2^6}, \dots\} = \begin{cases} 0 & \text{for } n \geq 1 \text{ odd,} \\ \frac{(A_{2n+1}^V)^4}{2^n} & \text{for } n \geq 0 \text{ even,} \end{cases} \quad (\text{A.37})$$

$$\begin{aligned} G_{n+2,n}(-\frac{1}{2}) &= \{\frac{1}{2}, \frac{1^3}{2^2}, \frac{1^3 \times 3}{2^3}, \frac{1 \times 3^3}{2^4}, \frac{3^3 \times 26}{2^5}, \frac{3 \times 26^3}{2^6}, \dots\} \\ &= \frac{1}{2^{n+1}} (A_{4[(n+2)/4]+1}^V)^{p(n+2)} (A_{4[n/4]+3}^V)^{p(n)}, \quad n \geq 0, \quad (\text{A.38}) \end{aligned}$$

where $p(n) = 1, 3, 3, 1$, if $(n - 4[\frac{n}{4}]) = 0, 1, 2, 3$, respectively.

Here A_n is a total number of $n \times n$ alternating sign matrices. Notations A_n^V , A_n^{VH} and A_n^{HT} stand, respectively, for numbers of vertically symmetric, vertically and horizontally symmetric and half turn symmetric $n \times n$ alternating sign matrices. Expressions for A_{2n+1}^V and $A_{4n \pm 1}^{VH}/A_{2n \pm 1}^V$ are given in (3.6) and (3.9). Formulas for A_n and A_n^{HT} are

$$A_n = \prod_{k=0}^{n-1} \frac{(3k+1)!}{(n+k)!}, \quad A_{2n}^{HT} = (A_n)^2 \prod_{k=0}^{n-1} \frac{3k+2}{3k+1}, \quad A_{2n+1}^{HT} = \prod_{k=1}^n \frac{4}{3} \left(\frac{(3k)!k!}{(2k)!^2} \right)^2. \quad (\text{A.39})$$

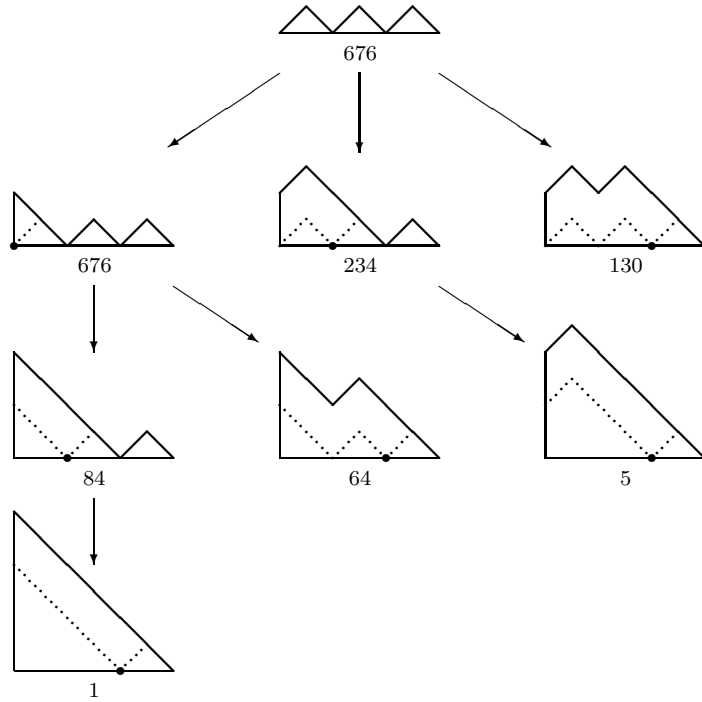
References

- [1] A.V. Razumov and Yu. G. Stroganov, "Spin chains and combinatorics", J. Phys. A: Math. Gen. **34** (2001) 3185–3190; arXiv:math.CO/0012141.
- [2] M. T. Batchelor, J. de Gier and B. Nienhuis, "The quantum symmetric XXZ chain at $\Delta = -1/2$, alternating sign matrices and plane partitions", J.Phys.A: Math. Gen. **34** (2001) L265-L270; arXiv:cond-mat/0101385.
- [3] A.V. Razumov and Yu. G. Stroganov, "Spin chains and combinatorics: twisted boundary conditions", J. Phys. A: Math. Gen. **34** (2001) 5335–5340; arXiv:math.CO/0102247.

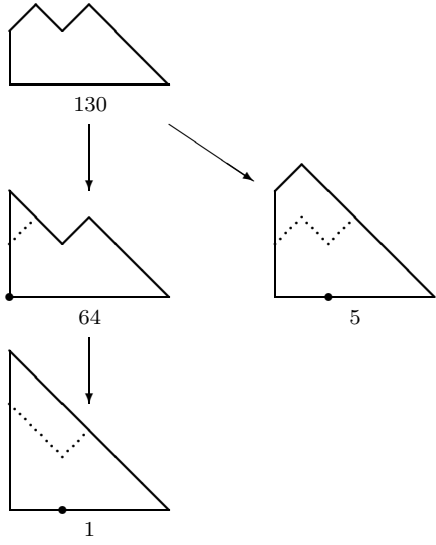
- [4] A.V. Razumov and Yu. G. Stroganov, "Combinatorial nature of ground state vector of $O(1)$ loop model", (2001) arXiv:math.CO/0104216.
- [5] P. A. Pearce, V. Rittenberg and J. de Gier, "Critical $Q = 1$ Potts Model and Temperley-Lieb Stochastic Processes", arXiv:cond-mat/0108051.
- [6] A.V. Razumov and Yu. G. Stroganov, "O(1) loop model with different boundary conditions and symmetry classes of alternating-sign matrices", (2001) arXiv:math.CO/0108103.
- [7] J. de Gier, M. T. Batchelor, B. Nienhuis and S. Mitra, "The XXZ spin chain at $\Delta = -1/2$: Bethe roots, symmetric functions and determinants", arXiv:math-ph/0110011.
- [8] M. T. Batchelor, J. de Gier and B. Nienhuis, "The Rotor Model and Combinatorics", Int. J. Mod. Phys. B **16** (2002) 1883-1890; arXiv:math-ph/0204002.
- [9] J. de Gier, B. Nienhuis, P. A. Pearce and V. Rittenberg, "Stochastic processes and conformal invariance", Phys. Rev. E **67** (2003) 016101-016104; arXiv:cond-mat/0205467.
- [10] P. A. Pearce, V. Rittenberg, J. de Gier and B. Nienhuis, "Temperley-Lieb stochastic processes", J. Phys. A Math. Gen. **35** (2002) L661-L668; arXiv:math-ph/0209017.
- [11] J. de Gier, "Loops, matchings and alternating-sign matrices", arXiv:math.CO/0211285.
- [12] J. de Gier, B. Nienhuis, P. A. Pearce and V. Rittenberg, "The raise and peel model of a fluctuating interface", J. Stat. Phys. **114** (2004) 1-35; arXiv:cond-mat/0301430.
- [13] S. Mitra, B. Nienhuis, J. de Gier and M. T. Batchelor, "Exact expressions for correlations in the ground state of the dense $O(1)$ loop model", arXiv:cond-mat/0401245.
- [14] I. de Gier, P. Pyatov and V. Rittenberg, "Magic in the XXZ spin chain" in preparation.
- [15] H. N. V. Temperley and E. Lieb, Proc. Roy Soc. London Ser. A **322** (1971) 251-280.
- [16] V. Pasquier and H. Saleur, "Common structures between finite systems and conformal field theories through quantum groups", Nucl.Phys. **B330** (1990), 523-556.
- [17] P. Martin and H. Saleur, Lett. Math. Phys. **30** (1994) 189-206.
- [18] P.P. Martin and D. Woodcock, J. Algebra **225** (2000) 957-988.
- [19] J. de Gier and P. Pyatov, "Bethe Ansatz for the Temperley-Lieb loop model with open boundaries", arXiv:hep-th/0312235.
- [20] R. Brak and J.W. Essam, "Asymmetric exclusion model and weighted lattice paths", arXiv:cond-mat/0311153.

- [21] F.C.Alcaraz, S.Dasmahapatra and V.Rittenberg, J. Phys. A: Math. Gen. **31** (1998) 845.
- [22] D.P. Robbins, ‘*Symmetry classes of alternating sign matrices*’. [arXiv:math.CO/0008045](https://arxiv.org/abs/math/0008045) (2000).
- [23] G. Kuperberg, ‘*Symmetry classes of alternating-sign-matrices under one roof*’. Ann. of Math. **156**, no. 3 (2002) 835–866; [arXiv:math.CO/0008184](https://arxiv.org/abs/math/0008184) (2000).
- [24] D.M. Bressoud, “*Proofs and Confirmations. The Story of the Alternating Sigh Matrix Conjecture*”, Cambridge University Press, Cambridge, 1999.
- [25] A. Zabrodin, “*A survey of Hirota’s difference equations*”, Theor. Mat. Fiz. **113** (1997) 1347–1392; [arXiv:solv-int/9704001](https://arxiv.org/abs/solv-int/9704001) (1997).

0-orbit, octet, sum over orbit = 170×11



2-orbit, quartet, sum over orbit = 50×4



4-orbit, doublet, sum over orbit = 6×1

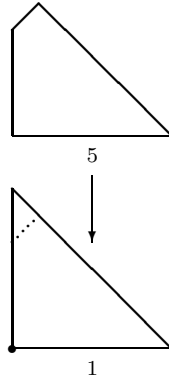
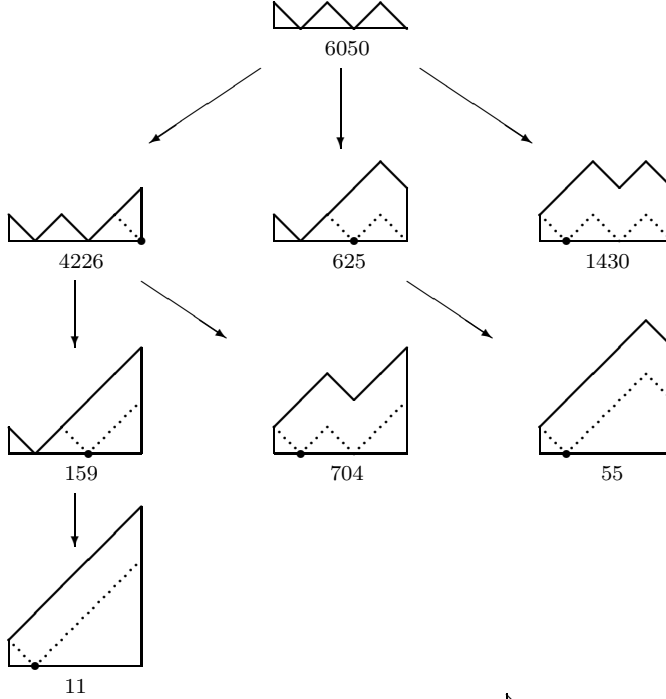


Figure 6: **Examples of maximal left orbits for size $L = 6$ Ballot paths.** Arrows on pictures point from source configurations to their coverings; bold dots indicate points where coverings happen; dashed lines show configuration before covering happen. Numbers standing below configurations are the corresponding stationary state coefficients in the case B RPM. Sums of the coefficients over orbits are described by the first one of relations (3.36).

$$0\text{-orbit, octet, sum over orbit} = \left(m_5^{(c)} S_7^{(a)} / S_5^{(a)}\right) \times p_5^{(b)} \left(\begin{array}{c} \text{triangle path} \end{array}\right) = 170 \times 78$$



$$1\text{-orbit, quartet, sum over orbit} = m_5^{(c)} \times p_6^{(b)} \left(\begin{array}{c} \text{triangle path} \end{array}\right) = 11 \times 676$$

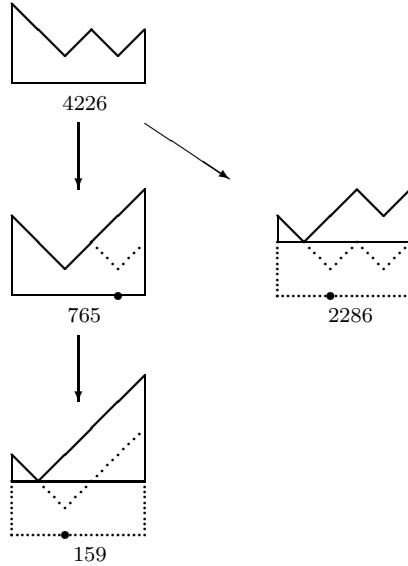


Figure 7: **Examples of maximal right orbits for size $L = 5$ Anchored Cross paths.** Notations are the same as on Fig.6. Numbers standing below configurations are the corresponding stationary state coefficients in case C RPM. On the last picture two configurations suffer from the total avalanche (3.30).

Diagram illustrating the relationship between numbers for $m=2n+3$ and $m=2n-1$ across different levels n .

The top row ($m=2n+3$) and bottom row ($m=2n-1$) are labeled with their respective values. The middle row ($n=2m+3$) and bottom row ($n=2m-1$) are labeled with their respective values.

The numbers are interconnected by lines, forming a branching pattern. The numbers are rational fractions, some with large denominators like 32, 16, 8, 4, and 2. The diagram is highly symmetric and shows a clear hierarchical structure.

Table 1: Particular solution (A.5), (A.6) of the Pascal’s hexagon relation (A.4). The numbers standing along indicated lines are given by formulas (A.10)–(A.13). Knowing them one can reconstruct data on the whole lattice by a repeated use of the Pascal’s hexagon relation.

$$\begin{aligned}
F_{4,2} &= 2xy + y^2 & F_{6,3} &= 11x^2y + 12xy^2 + 3y^3 \\
F_{5,2} &= 3x^2 + 6xy + 2y^2 & F_{7,3} &= 26x^3 + 78x^2y + 55xy^2 + 11y^3 \\
F_{6,2} &= 11x^2 + 12xy + 3y^2 & F_{8,3} &= 170x^3 + 294x^2y + 156xy^2 + 26y^3 \\
F_{7,2} &= 50x^2 + 30xy + 5y^2 & F_{9,3} &= 646x^3 + 816x^2y + 350xy^2 + 50y^3 \\
F_{8,2} &= 85x^2 + 42xy + 6y^2 \\
F_{9,2} &= 133x^2 + 56xy + 7y^2 \\
F_{8,4} &= 170x^3y + 294x^2y^2 + 156xy^3 + 26y^4 \\
F_{9,4} &= 646x^4 + 2584x^3y + 2839x^2y^2 + 1190xy^3 + 170y^4
\end{aligned}$$

$$\begin{aligned}
G_{2,2} &= 2 + 5x + 3x^2 & G_{3,2} &= 3 + 7x + 4x^2 \\
G_{2,3} &= 3 + 11x + 11x^2 & G_{3,3} &= 11 + 44x + 59x^2 + 26x^3 \\
G_{2,4} &= 4 + 19x + 26x^2 & G_{3,4} &= 26 + 137x + 255x^2 + 170x^3 \\
G_{2,5} &= 5 + 29x + 50x^2 & G_{3,5} &= 50 + 321x + 747x^2 + 646x^3 \\
G_{2,6} &= 6 + 41x + 85x^2 \\
G_{4,2} &= -4x - 9x^2 - 5x^3 \\
G_{4,3} &= 26 + 97x + 121x^2 + 50x^3 \\
G_{4,4} &= 170 + 935x + 1956x^2 + 1837x^3 + 646x^4 \\
G_{5,2} &= 5x + 16x^2 + 17x^3 + 6x^4 \\
G_{5,3} &= -50x - 179x^2 - 214x^3 - 85x^4 \\
G_{6,2} &= -6x - 19x^2 - 20x^3 - 7x^4
\end{aligned}$$

Table 2: Lattice polynomials $F_{m,n}(x, y)$ and $G_{m,n}(x)$ for small values of m and n .